

Constellation-Independent Range Estimation in Payload-Based OFDM-ISAC

Dongil Yang, *Student Member, IEEE*, Kaitao Meng, *Member, IEEE*, Christos Masouros, *Fellow, IEEE* and Kawon Han, *Member, IEEE*

Abstract—Orthogonal frequency division multiplexing (OFDM) is a key waveform for integrated sensing and communication (ISAC) due to its spectral efficiency and compatibility with modern wireless standards. In multi-target and clutter-rich environments, however, payload-based OFDM-ISAC can suffer from data-dependent sidelobes induced by non-constant-modulus modulation symbols. To overcome these limitations, this paper proposes a region-of-interest mismatched filter (ROI-MMF) that suppresses sidelobes within a prescribed delay region while preserving the mainlobe response. By leveraging the Woodbury identity, the proposed design admits an efficient closed-form implementation whose complexity scales with the ROI size rather than the number of subcarriers. We theoretically provide the ranging mean-square error (MSE) of the designed ROI-MMF, which shows the superior performance compared to conventional matched filtering (MF) and reciprocal filtering (RF) sensing receivers. Simulations across various constellations show that the proposed sensing receiver achieves a ranging MSE approaching the Cramér–Rao bound (CRB), which notably confirms that our design preserves the target ranging performance even under the non-constant-modulus constellation. Finally, the framework is experimentally validated with our over-the-air OFDM-ISAC testbed.

Index Terms—Cramér–Rao bound (CRB), ISAC, mean-square error (MSE), mismatched filtering, OFDM, range estimation.

I. INTRODUCTION

Integrated sensing and communication (ISAC) is a key enabling technology for future wireless systems, because communication and sensing can share the same spectrum, hardware, and signaling resources. Among candidate waveforms, orthogonal frequency division multiplexing (OFDM) is particularly attractive since it offers high spectral efficiency, is already adopted in modern communication standards [1], and remains well suited for joint communication and ranging due to its favorable sidelobe behavior under cyclic-prefix (CP) signaling [2]. As a result, OFDM-ISAC can add sensing capability to communication-centric wireless infrastructure without requiring major changes at the physical layer.

In OFDM-ISAC, one promising direction is to use communication data payloads directly for sensing. Since payload-based sensing exploits the full OFDM frame instead of relying only on dedicated reference signals such as preambles and pilots, it improves resource efficiency, coherent processing

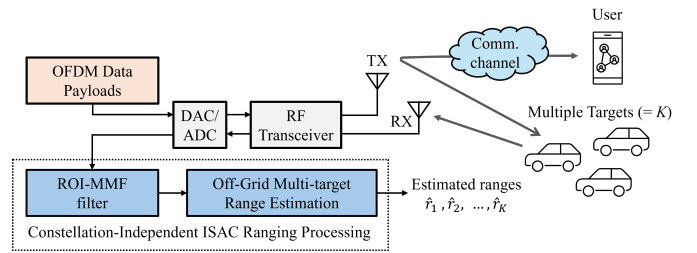


Fig. 1. Block diagram of the proposed constellation-independent OFDM-ISAC ranging processing, consisting of the ROI-MMF receiver and off-grid multi-target range estimation.

gain, range and Doppler ambiguities, resulting in better sensing accuracy [3]. The ranging performance is affected by the modulation constellation, especially under non-unit-amplitude signaling in multi-target and clutter-rich environments.

Two representative receivers for payload-based OFDM-ISAC are the matched filter (MF) and the reciprocal filter (RF) [4]. The MF preserves the original signal structure, but under non-constant-modulus constellations it produces data-dependent sidelobes [5]. These sidelobes increase inter-target interference and degrade delay estimation accuracy. On the other hand, the RF suppresses this sidelobe by inversely weighting the received signal with the transmitted symbols, but this operation amplifies noise with non-constant-modulus constellations. MF and RF therefore face two distinct but fundamental limitations. Recent work analyzed these effects in closed form: the MF ranging error is determined by the fourth-order moment of the constellation, while the RF error depends on its inverse second-order moment [6]. In other words, neither receiver approaches the Cramér–Rao bound (CRB) independently of the constellation once high-order modulation is used. While transmit signaling designs, such as ISAC constellation shaping [7]–[10] and constellation selection [11] may be adopted to overcome those limitations, they still introduce a performance trade-off between sensing and communications.

To address these limitations, we design a region-of-interest mismatched filter (ROI-MMF) for payload-based OFDM-ISAC ranging as shown in Fig. 1. Instead of suppressing unwanted responses across the whole delay domain, ROI-MMF suppresses sidelobes only within a prescribed ROI where target detection and estimation matter most, while preserving the mainlobe response so that the range estimation performance is maintained. This viewpoint is natural in practical sensing scenarios, since the target delay range is either known a priori or bounded by geometry in many deployments. By

D. Yang and K. Han are with the Department of Electrical Engineering, Ulsan National Institute of Science and Technology (UNIST), Ulsan, South Korea (emails: {dongil1223, kawon.han}@unist.ac.kr).

K. Meng is with the Department of Electrical and Electronic Engineering, University of Manchester, Manchester, UK.

C. Masouros is with the Department of Electronic and Electrical Engineering, University College London, London, UK.

confining the suppression to the ROI, the proposed receiver mitigates the data-dependent sidelobe of MF without incurring the severe inverse-symbol-power noise enhancement of RF, thereby enabling constellation-independent ranging behavior.

The main contributions of this paper are summarized as follows. First, we propose an ROI-based mismatched filtering framework for payload-based OFDM-ISAC that suppresses sidelobes over a prescribed delay region while preserving the mainlobe response. Second, we derive a closed-form solution via the Woodbury identity, whose complexity scales with the ROI size rather than the total number of subcarriers. Third, we develop a theoretical analysis under a multi-target environment and show that the proposed receiver approaches the CRB independently of the constellation, unlike MF and RF which suffer constellation-dependent penalties for target range estimation. Finally, we validate the proposed framework using numerical simulations across multiple constellations and measured OFDM-ISAC data.

II. SYSTEM MODEL

A. OFDM-ISAC Transmit Signal

We consider a monostatic OFDM-ISAC transceiver employing an OFDM waveform with N subcarriers. The subcarrier spacing is Δf , the total bandwidth is $B = N\Delta f$, and a cyclic prefix (CP) of duration T_{cp} is prepended to each OFDM symbol. The transmit vector is denoted as $\mathbf{x} = [x_0, x_1, \dots, x_{N-1}]^T \in \mathbb{C}^N$, whose entries are i.i.d. communication symbols drawn from a Q -ary constellation $\mathcal{C} = \{s_1, s_2, \dots, s_Q\}$. Without loss of generality, we assume the constellation is normalized to zero mean and unit average power, i.e., $\mathbb{E}[x_n] = 0$ and $\mathbb{E}[|x_n|^2] = 1$. In addition, each OFDM block is normalized such that $\|\mathbf{x}\|^2 = N$.

For the sensing performance analysis in Section III, we define two statistical moments of the constellation as $\mu_4 = \mathbb{E}[|x_n|^4]$ and $\nu_{-2} = \mathbb{E}[|x_n|^{-2}]$, which represent the fourth-order moment and the inverse second-order moment of the constellation, respectively [6]. For unit-modulus constellations such as PSK, both moments reduce to $\mu_4 = \nu_{-2} = 1$.

B. Sensing Signal Model

We consider K scatterers within the CP-induced unambiguous delay window. The k -th scatterer is characterized by a complex amplitude $\alpha_k \in \mathbb{C}$ and a round-trip delay τ_k , where α_k absorbs the path loss and the radar cross-section of the scatterer. The Doppler shift within one coherent processing interval (CPI) is assumed to be negligible relative to the subcarrier spacing, so that inter-carrier interference is avoided.

After CP removal and N -point FFT at the sensing receiver, the frequency-domain receive vector is modeled as

$$\mathbf{y} = \mathbf{a}^T \mathbf{H} \mathbf{X} + \mathbf{n}, \quad (1)$$

where $\mathbf{a} = [\alpha_1, \dots, \alpha_K]^T \in \mathbb{C}^K$ is the complex amplitude vector, $\mathbf{X} = \text{diag}(\mathbf{x}) \in \mathbb{C}^{N \times N}$ is the diagonal transmit symbol matrix, and $\mathbf{n} \sim \mathcal{CN}(\mathbf{0}, \sigma^2 \mathbf{I}_N)$ is additive white Gaussian noise. The delay-channel matrix $\mathbf{H} = [\mathbf{h}(\tau_1), \dots, \mathbf{h}(\tau_K)]^T \in \mathbb{C}^{K \times N}$ is composed of the delay steering vectors

$$\mathbf{h}(\tau) = [1, e^{-j2\pi\Delta f \tau}, \dots, e^{-j2\pi(N-1)\Delta f \tau}]^T. \quad (2)$$

The sensing SNR of the k -th scatterer is defined as $\text{SNR}_k = |\alpha_k|^2 / \sigma^2$. To process the sensing received signal, we apply a receive filter $\mathbf{w} \in \mathbb{C}^N$ to obtain $\mathbf{y}_{\text{out}} = \mathbf{w}^* \odot \mathbf{y}$.

III. PROPOSED ROI-MMF DESIGN FOR OFDM-ISAC

A. ROI-MMF Design

In many practical sensing scenarios, the target delays of interest are confined within a dedicated range, of which a bounded region can be determined by the deployment geometry. We therefore assume that all scatterers of interest are confined to a prescribed region of interest (ROI) in the delay domain,

$$\tau_k \in \mathcal{T} = [\tau_{\min}, \tau_{\max}], \quad k = 1, \dots, K, \quad (3)$$

with known boundaries τ_{\min} and τ_{\max} . Given the transmit block \mathbf{X} and the receive block \mathbf{Y} , our objective is to jointly estimate the number of scatterers K and the off-grid delay set $\{\tau_k\}_{k=1}^K$, while treating the complex amplitudes $\{\alpha_k\}$ as nuisance parameters.

To suppress data-dependent sidelobes within the ROI while preserving the mainlobe response, we design a mismatched filter $\mathbf{w} \in \mathbb{C}^N$ that minimizes the sidelobe energy across a finite set of delay shifts covering \mathcal{T} , subject to a unit-gain constraint on the transmit vector \mathbf{x} .

Let M_{\max} denote the largest delay shift (in bin units) corresponding to \mathcal{T} . We denote the bilateral shift set as

$$\mathcal{S} = \{-M_{\max}, \dots, -1\} \cup \{1, \dots, M_{\max}\}, \quad (4)$$

with cardinality $|\mathcal{S}| = 2M_{\max}$. For each $m \in \mathcal{S}$, we define the shifted steering vector $[\mathbf{e}_m]_n = e^{j2\pi mn/N}$ and the shifted transmit replica $\mathbf{z}_m = \mathbf{x} \odot \mathbf{e}_m \in \mathbb{C}^N$. Multiplication by \mathbf{e}_m in the frequency domain corresponds to a circular delay shift by m bins in the time domain, so \mathbf{z}_m represents the frequency-domain response that the receiver would observe from a target at delay shift m relative to the mainlobe. Stacking the replicas yields the off-target steering matrix $\mathbf{Z} = [\mathbf{z}_1, \mathbf{z}_2, \dots, \mathbf{z}_{2M_{\max}}] \in \mathbb{C}^{N \times |\mathcal{S}|}$. Consequently, $\|\mathbf{Z}^H \mathbf{w}\|_2^2 = \sum_{m \in \mathcal{S}} |\mathbf{w}^H \mathbf{z}_m|^2$ measures the total sidelobe energy across the prescribed off-target shift set.

With this ROI in hand, the ROI-MMF design problem is formulated as

$$\min_{\mathbf{w}} \|\mathbf{Z}^H \mathbf{w}\|_2^2 + \lambda \|\mathbf{w}\|_2^2 \quad \text{s.t.} \quad \mathbf{w}^H \mathbf{x} = N, \quad (5)$$

where the first term penalizes the sidelobe energy within \mathcal{S} , the second term is a ridge penalty that controls noise enhancement, and the constraint fixes the mainlobe gain. The regularization parameter $\lambda > 0$ governs the trade-off between sidelobe suppression and noise enhancement. Notably, the formulated problem in (5) can have a closed-form solution, which is efficiently obtained by utilizing the Woodbury identity as follows.

Theorem 1. *The unique solution to (5) is given by*

$$\mathbf{w}_{\text{ROI}} = \frac{N}{\tilde{\mathbf{w}}^H \mathbf{x}} \tilde{\mathbf{w}}, \quad \tilde{\mathbf{w}} = \frac{1}{\lambda} \left(\mathbf{x} - \mathbf{Z}(\lambda \mathbf{I}_{|\mathcal{S}|} + \mathbf{Z}^H \mathbf{Z})^{-1} \mathbf{Z}^H \mathbf{x} \right), \quad (6)$$

which requires only the inversion of an $|\mathcal{S}| \times |\mathcal{S}|$ matrix.

Proof. The KKT stationarity condition of (5) yields $(\mathbf{Z} \mathbf{Z}^H + \lambda \mathbf{I}_N) \mathbf{w} = \beta \mathbf{x}$, which requires inverting an $N \times N$ matrix. Applying the Woodbury identity

$$(\lambda \mathbf{I}_N + \mathbf{Z} \mathbf{Z}^H)^{-1} = \frac{1}{\lambda} \mathbf{I}_N - \frac{1}{\lambda} \mathbf{Z}(\lambda \mathbf{I}_{|\mathcal{S}|} + \mathbf{Z}^H \mathbf{Z})^{-1} \mathbf{Z}^H \quad (7)$$

reduces the inversion to an $|\mathcal{S}| \times |\mathcal{S}|$ system. Enforcing the gain constraint $\mathbf{w}^H \mathbf{x} = N$ yields (6). ■

Theorem 1 indicates that the computational complexity of the ROI-MMF design scales with the ROI size $|\mathcal{S}|$ rather than the total number of subcarriers N . For ROIs of practical interest with $|\mathcal{S}| < N$, this provides a substantial reduction compared to a direct inversion of the full $N \times N$ matrix.

B. Theoretical Performance Analysis of ROI-MMF

We now analyze the delay estimation MSE of the ROI-MMF receiver and compare it against the MF and RF baselines. For a general filter \mathbf{w} , let $g_n = w_n^* x_n$ denote the effective product, and define the sidelobe as

$$c_m = \frac{1}{N} \sum_{n=0}^{N-1} g_n e^{j2\pi mn/N} = \frac{1}{N} \mathbf{w}^H \mathbf{z}_m, \quad (8)$$

where the normalized filter gives $c_0 = 1$. For K targets with delays $\{\tau_k\}_{k=1}^K$, following the asymptotic estimator framework of [6], the per-target delay estimation MSE under filter \mathbf{w} admits the unified form

$$\text{MSE}_k = \frac{I_k(\mathbf{w}) + N_k(\mathbf{w})}{2(2\pi\Delta f)^2 |\alpha_k|^2 (\sum_n n^2 \mathbb{E}[g_n])^2}, \quad (9)$$

where $I_k(\mathbf{w}) = \sum_{j \neq k} |\alpha_j|^2 \text{Var}(B_{k,j})$ with $B_{k,j} = \sum_n n g_n e^{j2\pi n \xi_{k,j}}$ and $\xi_{k,j} = \Delta f(\tau_k - \tau_j)$ captures the aggregate interference variance from the other $K - 1$ targets, and $N_k(\mathbf{w}) = \sigma^2 \mathbb{E}[\sum_n n^2 |w_n|^2]$ captures the noise enhancement. The gain constraint $\mathbf{w}^H \mathbf{x} = N$ holds deterministically by construction and, together with the i.i.d. symmetry of $\{x_n\}$ across subcarriers, yields $\mathbb{E}[g_n] = 1$ for all n , so the denominator of (9) reduces to $(\sum_n n^2)^2$.

1) *MF and RF baselines:* For the matched filter $\mathbf{w}_{\text{MF}} = \mathbf{x}$ and the reciprocal filter $\mathbf{w}_{\text{RF}} = 1/\mathbf{x}^*$, specializing (9) recovers the closed-form expressions [6]

$$\text{MSE}_{\text{MF},k} = \frac{3[(\mu_4 - 1) \sum_{j \neq k} |\alpha_j|^2 + \sigma^2]}{8\pi^2 \Delta f^2 |\alpha_k|^2 N^3}, \quad (10)$$

$$\text{MSE}_{\text{RF},k} = \frac{3\sigma^2 \nu_{-2}}{8\pi^2 \Delta f^2 |\alpha_k|^2 N^3}. \quad (11)$$

The MF MSE is μ_4 -limited through data-dependent sidelobes, while the RF MSE is ν_{-2} -limited through noise enhancement. Neither achieves the CRB under non-constant-modulus constellations.

2) *ROI-MMF:* To analyze the ranging MSE of the proposed ROI-MMF under random communication signals, we first provide an energy identity for the ROI-MMF that bounds both its residual sidelobe energy and filter norm. These bounds will serve as the analytical anchors for the interference and noise-enhancement analysis developed throughout this subsection.

Lemma 1. *The ROI-MMF solution (6) satisfies*

$$\|\mathbf{Z}^H \mathbf{w}_{\text{ROI}}\|_2^2 \leq \frac{\lambda N}{1 - \rho_S}, \quad \|\mathbf{w}_{\text{ROI}}\|_2^2 \leq \frac{N}{1 - \rho_S}, \quad (12)$$

where $\rho_S = \frac{1}{N} \mathbf{x}^H \mathbf{Z}(\lambda \mathbf{I}_{|\mathcal{S}|} + \mathbf{Z}^H \mathbf{Z})^{-1} \mathbf{Z}^H \mathbf{x} \in [0, 1)$.

Proof. Substituting $\mathbf{w}_{\text{ROI}} = \beta(\mathbf{Z}\mathbf{Z}^H + \lambda \mathbf{I}_N)^{-1} \mathbf{x}$ into the gain constraint and applying the Woodbury identity yields $\beta = \lambda/(1 - \rho_S)$. Left-multiplying the KKT equation by $\mathbf{w}_{\text{ROI}}^H$ and using $\mathbf{w}_{\text{ROI}}^H \mathbf{x} = N$ gives $\|\mathbf{Z}^H \mathbf{w}_{\text{ROI}}\|_2^2 + \lambda \|\mathbf{w}_{\text{ROI}}\|_2^2 = \beta N$, from which (12) follows. ■

Lemma 1 indicates that the residual sidelobe energy and the filter norm of the ROI-MMF are jointly controlled by the single quantity ρ_S , with the regularization parameter λ governing the trade-off between the two.

Moreover, the following lemma characterizes the ROI-MMF noise enhancement in closed form.

Lemma 2. *Define $\delta_{\text{ROI}}^{(N)} = \|\mathbf{w}_{\text{ROI}}\|_2^2/N$ so that $N_k(\mathbf{w}_{\text{ROI}}) = \sigma^2 \delta_{\text{ROI}}^{(N)} \sum_n n^2$. In the regime $\lambda \ll N$ and $|\mathcal{S}| < N$,*

$$\delta_{\text{ROI}}^{(N)} = \frac{N}{N - \kappa_2 |\mathcal{S}|}, \quad (13)$$

where $\kappa_2 = \mathbb{E}[(|x_n|^2 - 1)^2]$ is the centered second moment of the constellation. The excess factor $\kappa_2 |\mathcal{S}|/N$ is bounded above by a small constant under $|\mathcal{S}| < N$ and is independent of the inverse second moment ν_{-2} .

Proof. With $\mathbf{X} = \text{diag}(\mathbf{x})$ and $\mathbf{V} = [\mathbf{e}_{m_1}, \dots, \mathbf{e}_{m_{|\mathcal{S}|}}]$, we have $\mathbf{Z} = \mathbf{X}\mathbf{V}$. Writing $|x_n|^2 = 1 + u_n$ with $u_n = |x_n|^2 - 1$ and using the Vandermonde orthogonality $\mathbf{V}^H \mathbf{V} = N \mathbf{I}_{|\mathcal{S}|}$, we obtain

$$\mathbf{Z}^H \mathbf{Z} = N \mathbf{I}_{|\mathcal{S}|} + \boldsymbol{\varepsilon}, \quad \boldsymbol{\varepsilon} = \mathbf{V}^H \text{diag}(u_n) \mathbf{V},$$

where $\boldsymbol{\varepsilon}$ is a zero-mean Hermitian perturbation since $\mathbb{E}[u_n] = 0$. Setting $\xi = \lambda + N$ and $\mathbf{q} = \mathbf{Z}^H \mathbf{x}$, the quantity ρ_S from Lemma 1 can be rewritten as $\rho_S = \mathbf{q}^H (\xi \mathbf{I} + \boldsymbol{\varepsilon})^{-1} \mathbf{q}/N$. From the energy identity (12), $\|\mathbf{w}_{\text{ROI}}\|_2^2 = N/(1 - \rho_S) - \|\mathbf{Z}^H \mathbf{w}_{\text{ROI}}\|_2^2/\lambda$. The correction term $\|\mathbf{Z}^H \mathbf{w}_{\text{ROI}}\|_2^2/\lambda$ is of order λ and is negligible in the regime $\lambda \ll N$. Hence $\|\mathbf{w}_{\text{ROI}}\|_2^2 \approx N/(1 - \rho_S)$, and $\delta_{\text{ROI}}^{(N)} \approx 1/(1 - \rho_S)$.

In the regime given that $|\mathcal{S}| < N$, the spectral-norm bound $\|\boldsymbol{\varepsilon}\|/\xi \leq C\sqrt{|\mathcal{S}|/N} < 1$ holds for a constant C independent of N . A Neumann-series expansion of $(\xi \mathbf{I} + \boldsymbol{\varepsilon})^{-1}$ therefore converges, and the leading term gives $\rho_S \approx \mathbf{q}^H \mathbf{q}/(N\xi)$. Concentration of $\mathbf{q}^H \mathbf{q}$ around its mean, combined with $\mathbb{E}[\mathbf{q}^H \mathbf{q}] = |\mathcal{S}|N\kappa_2$ and $\lambda \ll N$, yields $\rho_S \approx \kappa_2 |\mathcal{S}|/N$, leading to (13). ■

Remark 1. The noise enhancement of ROI-MMF depends on the constellation only through the centered moment κ_2 of $|x_n|^2$, which remains bounded for QAM formats ($\kappa_2 \rightarrow 0.40$ as $M \rightarrow \infty$). This is in sharp contrast to the RF receiver, whose noise penalty ν_{-2} grows unboundedly as constellation points approach the origin.

Building on Lemma 1 and Lemma 2, we are now ready to derive a closed-form expression for the MSE of the ROI-MMF as the following theorem states.

Theorem 2 (ROI-MMF delay estimation MSE). *The closed-form expression of the ROI-MMF delay estimation MSE is approximately given by*

$$\text{MSE}_{\text{ROI},k} = \frac{3\sigma^2}{8\pi^2 \Delta f^2 |\alpha_k|^2 N^3} \cdot \delta_{\text{ROI}}, \quad (14)$$

with $\delta_{\text{ROI}} = \delta_{\text{ROI}}^{(N)} + \delta_{\text{ROI}}^{(I)}$.

Proof. Let $\rho_{\text{tot}} = \sum_{j \neq k} |\alpha_j|^2/\sigma^2$ denote the aggregate interference SNR. The interference residual of the ROI-MMF, defined as $\delta_{\text{ROI}}^{(I)} = \sum_{j \neq k} |\alpha_j|^2 \text{Var}(B_{k,j}^{\text{ROI}})/(\sigma^2 \sum_n n^2)$ such that $I_k(\mathbf{w}_{\text{ROI}}) = \sigma^2 \delta_{\text{ROI}}^{(I)} \sum_n n^2$, satisfies

$$\delta_{\text{ROI}}^{(I)} \leq \frac{\rho_{\text{tot}} \lambda}{N(1 - \rho_S)}, \quad (15)$$

which follows from the suppression property $\sum_{m \in \mathcal{S}} |c_m|^2 \leq \lambda/(N(1 - \rho_S))$ established in Lemma 1 together with an

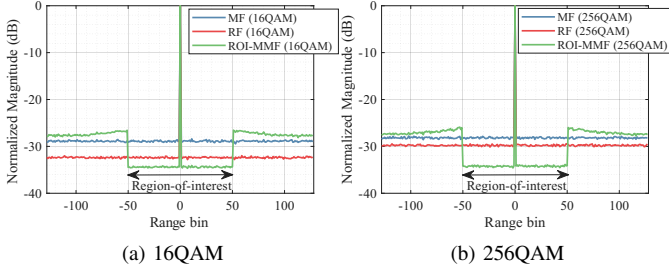


Fig. 2. Normalized range profiles of the MF, RF, and the proposed ROI-MMF receivers under (a) 16-QAM and (b) 256-QAM at a target SNR of 10 dB.

application of the Cauchy–Schwarz inequality. The bound (15) is structurally controlled by the design parameter λ and vanishes as $\lambda \rightarrow 0$. Combining this interference residual with the noise enhancement $\delta_{\text{ROI}}^{(N)}$ characterized in Lemma 2 and substituting into the unified form (9) yields (14). ■

3) *Performance Comparisons:* Applying the standard Fisher information analysis yields the per-target CRB as $\text{CRB} = \frac{\sigma^2}{8\pi^2 \Delta f^2 |\alpha_k|^2 \sum_n n^2}$ [6]. To compare the ranging performance of MF, RF, and ROI-MMF, we introduce the estimation efficiency defined as $\eta = \text{RMSE}/\sqrt{\text{CRB}}$. Then, dividing (10), (11), and (14) yields

$$\eta_{\text{MF}} = \sqrt{1 + (\mu_4 - 1)\rho_{\text{tot}}}, \quad \eta_{\text{RF}} = \sqrt{\nu_{-2}}, \quad \eta_{\text{ROI}} = \sqrt{\delta_{\text{ROI}}}, \quad (16)$$

where $\rho_{\text{tot}} = \sum_{j \neq k} |\alpha_j|^2 / \sigma^2$ is the aggregate interference SNR introduced above. Unlike MF and RF whose estimation efficiency scales according to μ_4 and ν_{-2} of the constellation, the ROI-MMF shows the superior performance less affected by the modulation constellation geometry, which is shown in the following corollary.

Corollary 1. *In the regime $\lambda \ll N$ and $|\mathcal{S}| \ll N$, the ROI-MMF estimation efficiency η_{ROI} nearly approaches unity independently of the constellation geometry,*

Proof. From (16), $\eta_{\text{ROI}}^2 = \delta_{\text{ROI}} = \delta_{\text{ROI}}^{(N)} + \delta_{\text{ROI}}^{(I)}$. By Lemma 2 and (15), $\delta_{\text{ROI}}^{(N)} \approx 1 + \kappa_2 |\mathcal{S}|/N$ and $\delta_{\text{ROI}}^{(I)} \leq \rho_{\text{tot}} \lambda / N$, so δ_{ROI} deviates from unity only by $\kappa_2 |\mathcal{S}|/N + \rho_{\text{tot}} \lambda / N$ in the stated regime. As the centered moment κ_2 saturates to a small constant, δ_{ROI} remains close to unity and constellation-independent. ■

Remark 2. The constellation-independent property of ROI-MMF stems from the fact that δ_{ROI} depends on the constellation only through the centered moment κ_2 multiplied by $|\mathcal{S}|/N \ll 1$, and through the factor $\rho_{\text{tot}} \lambda / N$ which is structurally controlled by λ . In contrast, the MF penalty grows with μ_4 (the fourth-order moment) and the RF penalty grows with ν_{-2} (the inverse second-order moment). The advantage of ROI-MMF over the classical receive filters therefore widens as the constellation moves away from constant modulus.

IV. NUMERICAL SIMULATIONS AND EXPERIMENTATION

In this section, we validate the proposed theory and the closed-form analysis through numerical simulations and a proof-of-concept (PoC) demonstration. To examine the impact of the modulation constellation on the sensing performance, we consider various constellations: QPSK, 16-QAM, 64-QAM, and 256-QAM.

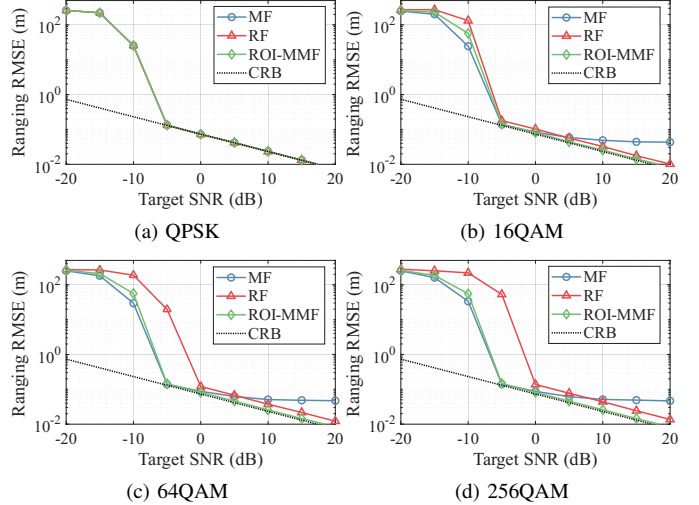


Fig. 3. Range estimation RMSE versus target SNR for the MF, RF, and the proposed ROI-MMF under (a) QPSK, (b) 16-QAM, (c) 64-QAM, and (d) 256-QAM modulation. $N = 256$, $L = 8$, $\lambda = 0.1$, and $\mathcal{S} = \{\pm 1, \dots, \pm 50\}$.

A. Numerical Simulation Results

For the numerical simulations, we adopt a CP-OFDM waveform with $N = 256$, $B = 50$ MHz, and a CP length of $0.64 \mu\text{s}$. We coherently process L number of OFDM symbols in one CPI, of which value is $L = 8$. The proposed ROI-MMF is configured with the bilateral shift set $\mathcal{S} = \{-50, \dots, -1\} \cup \{1, \dots, 50\}$, corresponding to the range interval of -150 m to 150 m, and regularization parameter $\lambda = 0.1$. Each result is averaged over 2,000 Monte-Carlo runs. A subspace-based matrix pencil (MP) estimator is employed for off-grid range estimation [12], with the number of scatterers K determined by a multi-layer perceptron (MLP)-based model-order selection.

We first examine the structural difference between the three receivers through their range profiles. Fig. 2 shows the normalized range profiles of MF, RF, and ROI-MMF under 16-QAM and 256-QAM at a target SNR of 10 dB with a single scatterer. The MF profile exhibits a constellation-dependent sidelobe floor that increases with the modulation order, since its sidelobe energy is governed by the fourth moment μ_4 . The RF profile suppresses the sidelobes but lifts the noise floor as ν_{-2} grows with the modulation order in the case of QAM. The proposed ROI-MMF, in contrast, forms a clear notch across the prescribed ROI for both constellations, and the two profiles nearly overlap, which confirms the constellation-independent suppression behavior predicted by Lemma 2.

Next, we evaluate the multi-target ranging accuracy. Two scatterers are placed at off-grid ranges $r_1 = 60.9$ m and $r_2 = 90.9$ m within the ROI, and $L = 8$ consecutive OFDM symbols are collected within one CPI. Fig. 3 shows the range estimation RMSE versus the target SNR for the four constellations, together with the CRB. For QPSK, all three filters coincide with the CRB, in agreement with Corollary 1. For non-constant-modulus constellations, the MF curves saturate as the SNR increases, since the sidelobe interference from the other target dominates the estimation error, consistent with the μ_4 -limited expression (10). The RF curves exhibit a constant gap from the CRB whose magnitude grows with ν_{-2} , matching (11). In contrast, the proposed ROI-MMF tracks the CRB

Table I
THE VALUES OF THEORETICAL AND NUMERICAL $\eta = \text{RMSE}/\sqrt{\text{CRB}}$ FOR MF, RF, AND ROI-MMF UNDER VARIOUS CONSTELLATIONS.

Const.	MF		RF		ROI-MMF	
	Theory	Numer.	Theory	Numer.	Theory	Numer.
QPSK	1.000	1.013	1.000	1.013	1.000	1.013
16QAM	2.049	2.102	1.374	1.398	1.069	1.095
32QAM	2.025	2.013	1.491	1.485	1.067	1.098
64QAM	2.193	2.188	1.638	1.607	1.084	1.102
128QAM	2.105	2.071	1.730	1.734	1.075	1.099
256QAM	2.225	2.212	1.850	1.894	1.087	1.115

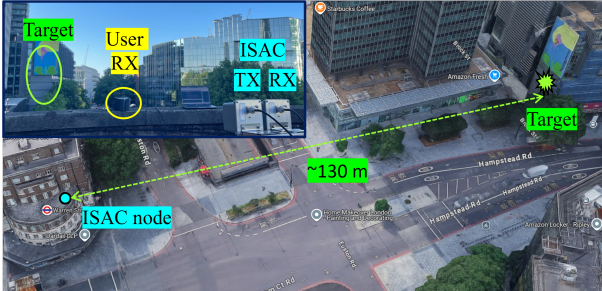


Fig. 4. Photograph of the measurement setup.

across all constellations and SNRs.

Table I reports the estimation efficiency η at SNR = 10 dB, comparing the closed-form predictions (16) against the simulated values across QPSK through 256-QAM. The closed-form expressions closely match the simulated estimation results, providing numerical validation of the constellation-independent behavior established in Corollary 1.

B. Experimental Results

Beyond numerical simulations, we further validate the proposed receiver design and its theory through over-the-air experiments. To this end, a software-defined radio (AD9363) with directional antennas of 12 dBi gain is employed. The center frequency is set to 2.4 GHz with a bandwidth of $B = 20$ MHz and $N = 512$ subcarriers. In addition, 512 OFDM symbols are transmitted per frame. The ROI is set to [50, 250] m to cover the deployment geometry of interest, and each measurement result is obtained by averaging over 100 independent frames. The desired target, a building wall with high reflectivity, is located approximately 130 m from the ISAC node, as illustrated in Fig. 4.

Fig. 5 shows the measured range profiles under 16-QAM and a customized 32-APSK modulation. As predicted by the analysis, the MF profile suffers from elevated data-dependent sidelobes that mask the desired target peak. The RF profile suppresses these sidelobes but lifts the overall noise floor. The proposed ROI-MMF effectively suppresses the response within the prescribed ROI while preserving the target peak at ~ 130 m, achieving the highest in-ROI dynamic range for both constellations. This experimentally confirms that the constellation-independent ranging property established theoretically also carries over to practical over-the-air deployments.

V. CONCLUSION

In this paper, we have proposed a ROI-MMF for payload-based OFDM-ISAC ranging, which suppresses data-dependent

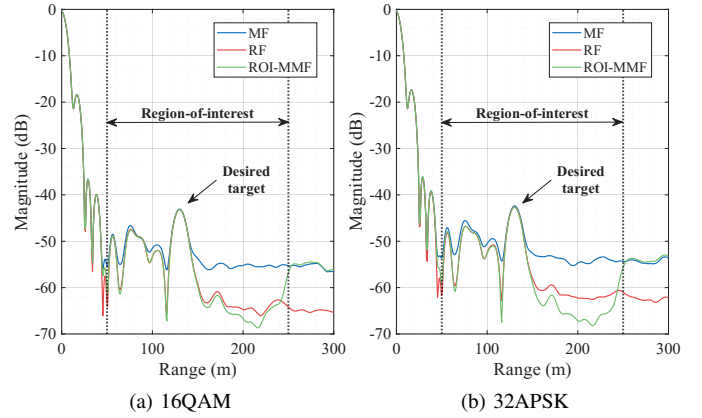


Fig. 5. Measured range profiles of the MF, RF, and ROI-MMF receivers under (a) 16-QAM and (b) customized 32-APSK modulation.

sidelobes within a prescribed delay region while preserving the mainlobe response and admits a closed-form solution via the Woodbury identity. Through an estimation-theoretic analysis, we have shown that the proposed receiver strictly dominates the conventional filters and nearly approaches the CRB independently of the modulation constellation. The theoretical findings are validated through numerical simulations and over-the-air measurements, providing a constellation-independent receive-filter framework.

REFERENCES

- [1] R. Prasad, *OFDM for wireless communications systems*. Artech House, 2004, vol. 2.
- [2] F. Liu, Y. Zhang, Y. Xiong, S. Li, W. Yuan, F. Gao, S. Jin, and G. Caire, "CP-OFDM achieves the lowest average ranging sidelobe under QAM/PSK constellations," *IEEE Trans. Inf. Theory*, 2025.
- [3] C. Sturm and W. Wiesbeck, "Waveform design and signal processing aspects for fusion of wireless communications and radar sensing," *Proc. IEEE*, vol. 99, no. 7, pp. 1236–1259, 2011.
- [4] M. F. Keskin, M. M. Mojahedian, J. O. Lacruz, C. Marcus, O. Eriksson, A. Giorgetti, J. Widmer, and H. Wymeersch, "Fundamental trade-offs in monostatic ISAC: A holistic investigation towards 6G," *IEEE Trans. Wireless Commun.*, 2025.
- [5] F. Liu, Y. Xiong, S. Lu, S. Li, W. Yuan, C. Masouros, S. Jin, and G. Caire, "Uncovering the iceberg in the sea: Fundamentals of pulse shaping and modulation design for random ISAC signals," *IEEE Transactions on Signal Processing*, 2025.
- [6] K. Han, K. Meng, A. Chatzicharistou, and C. Masouros, "Constellation Design in OFDM-ISAC over Data Payloads: From MSE Analysis to Experimentation," to appear in *2026 IEEE International Conference on Communications*, 2026.
- [7] K. Han, C. Masouros, T. Riihonen, and M. G. Amin, "Next-Generation MIMO Transceivers for Integrated Sensing and Communications: Unique Security Vulnerabilities and Solutions," *arXiv preprint arXiv:2511.20309*, 2025.
- [8] B. Geiger, F. Liu, S. Lu, A. Rode, D. G. Gavia, C. Muth, and L. Schmalen, "Constellation Shaping for OFDM-ISAC Systems: From Theoretical Bounds to Practical Implementation," *IEEE Transactions on Communications*, 2026.
- [9] Z. Du, J. Xu, Y. Xiong, J. Wang, M. F. Keskin, H. Wymeersch, F. Liu, and S. Jin, "Probabilistic constellation shaping for OFDM ISAC signals under temporal-frequency filtering," *IEEE Transactions on Wireless Communications*, 2026.
- [10] Z. Du, F. Liu, Y. Xiong, T. X. Han, Y. C. Eldar, and S. Jin, "Reshaping the ISAC tradeoff under OFDM signaling: A probabilistic constellation shaping approach," *IEEE Trans. Signal Process.*, 2024.
- [11] K. Meng, K. Han, C. Masouros, and F. Liu, "Constellation Selection and Power Control for OFDM-based ISAC: From Theory to Prototype," *arXiv preprint arXiv:2603.03895*, 2026.
- [12] T. K. Sarkar and O. Pereira, "Using the matrix pencil method to estimate the parameters of a sum of complex exponentials," *IEEE Antennas and propagation Magazine*, vol. 37, no. 1, pp. 48–55, 1995.